Dalton Transactions

An international journal of inorganic chemistry

Accepted Manuscript

This article can be cited before page numbers have been issued, to do this please use: E. Abás, R. Pena-Martínez, D. Aguirre-Ramírez, A. Rodríguez Diéguez, M. Laguna and L. Grasa, *Dalton Trans.*, 2020, DOI: 10.1039/C9DT04423J.

This is an Accepted Manuscript, which has been through the Royal Society of Chemistry peer review process and has been accepted for publication.

Accepted Manuscripts are published online shortly after acceptance, before technical editing, formatting and proof reading. Using this free service, authors can make their results available to the community, in citable form, before we publish the edited article. We will replace this Accepted Manuscript with the edited and formatted Advance Article as soon as it is available.

You can find more information about Accepted Manuscripts in the Information for Authors.

Please note that technical editing may introduce minor changes to the text and/or graphics, which may alter content. The journal's standard Terms & Conditions and the Ethical guidelines still apply. In no event shall the Royal Society of Chemistry be held responsible for any errors or omissions in this Accepted Manuscript or any consequences arising from the use of any information it contains.

ROYAL SOCIETY OF CHEMISTRY

rsc.li/dalton

View Article Online
DOI: 10.1039/C9DT04423J

ARTICLE

New selective thiolate gold(I) complexes inhibit proliferation of different human cancer cells and induce apoptosis in primary cultures of mouse colon tumors

Elisa Abas,[a] Raquel Pena-Martinez,[a] Diego Aguirre-Ramírez,[b] Antonio Rodriguez-Dieguez,[e] Mariano Laguna,*[,a] and Laura Grasa*[,b,c,d]

New thiolate gold(I) complexes with $P(NMe_2)_3$ (HMPT) as a phosphane group have been synthesized [Au(SR)(HMPT)] (R= Spy, Spyrim, SMe_2pyrim, Sbenzothiazole, Sthiazoline, Sbenzimidazole and 2-thiouracil). All of them have been characterized, including X-Ray studies of complexes with SMe_2pyrim, Sbenzothiazole and 2-thiouracil moieties. In addition, their potential application as anticancer drugs has been analyzed by determining their pharmacokinetic activity (water solubility, cell permeability and BSA transport protein affinity). Based on the good results of these experiments, we carried out studies of cell viability with our compounds on different cell lines (A2780, A2780R and Caco-2/TC7 cells), showing more cytotoxic activity than cisplatin in all cases. Besides, two of the synthesized complexes exhibited specific selectivity for cancerous Caco-2 cells, arising complexes with Sbenzimidazole and 2-thiouracil groups, as potential candidates for anticancer drugs. These complexes were able to induce a strong inhibition of the thioredoxin reductase (TrxR) protein and oxidative damage in membrane lipids. Additional studies in primary cultures from mouse colon tumors showed that these two complexes are proapoptotic by the exposure of phosphatidylserine. Based on our results, we conclude that two of our thiolate gold(I) complexes are good and effective candidates to be used in chemotherapy.

Introduction

The human body, as every living organism, is composed of millions of cells in a continuous process of growing, dividing and dying. This process, known as cell cycle, is tightly controlled by several check points which ensure the correct DNA replication, but sometimes a mutation can be omitted and corrupted DNA proliferates. Mutations can be inherited, which suppose only the 10% of mutations, or be a result of DNA damage by environmental factors, such as the harmful substances in tobacco smoke (chemical carcinogens), UV radiation from sunlight (physical carcinogens) or the human papillomavirus (biological carcinogens).[1] These mutations usually imply tumorgenesis.[2, 3] Thus, as it can be inhered the more cell proliferation processes the more sensitive the tissue is. This is why colorectal cancer (CRC) is the third most commonly diagnosed cancer and the second highest cause of cancer death in 2018,[4, 5] because up to 10^{10} cells are daily replaced in a human colon.[6] Nowadays, there is still not a drug capable to fight against cancer by itself and two or more drugs are required to struggle the uncontrolled proliferation of cancer cells. Based on this fact, one of the most urgent objectives of medicinal chemistry is the discovery of novel and more effective and selective drugs against cancer. Bioinorganic chemistry already provides different examples of metal complex-based drugs whose antitumor activity is well known: among them, cisplatin is one of the most frequently used clinical anticancer drugs. Much has been researched since the discovery of cisplatin, and as a result new generations of platinum based drugs have been developed. One of them, oxaliplatin is still used in the treatment of CRC, in combination with 5-fluoracil and leucovin (FOLFOX).[7] Nevertheless, platinum drugs are well known due to their lack of selectivity and their severe side effects. It is believed that both facts are closely related and based on the mechanism of action. DNA is the main target for platinum drugs, but these compounds not only damage the DNA present in cancer but also in normal cells. Therefore, scientists are focused on the development of new organometallic complexes as effective as platinum but more selective, what means complexes mechanistically different. Although different metals would be able to be good candidates, the therapeutic use of gold and its complexes dates back to medieval ages and the Renaissance.[8] Despite this, the synthesis of new derivates based on gold for chemotherapy is still a developing area of medicinal and pharmaceutical chemistry.[9-12] Application of gold complexes is expanded from their use in rheumatoid arthritis treatment until their employ as antimalarial agents and now in chemotherapy.[13] The most widely known gold complex with pharmacological properties is auranofin, which represents an important milestone in the development of anticancer drugs based on Au(I)–phosphane complexes.[14-20] Auranofin's structure has served as a model to new gold drugs, where gold(I) center presents two different bonds, one to the S-

atom of the thioglucose, and another one to the P-atom of the phosphane moiety (**Figure 1**). Owing to the soft acidic nature of gold(I), it is understandable that the gold(I) center is coordinated to these atoms, well known to be typical soft bases.

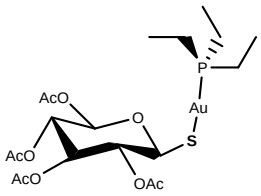

Figure 1. Structure of auranofin.

Phosphorus- and Sulphur-containing nucleophiles are widely used as ligands to enhance the stability of the resulting gold(I) complexes under physiological conditions, that is why the phosphanegold(I) thiolate derivatives constitute a family of very promising experimental agents for cancer treatment.[11, 19, 21, 22] In addition to the chemical issue, the coordination sphere of the metallic center has to be carefully selected in order to give good physicochemical properties to the final complex, like water solubility and lipophilicity among others. In fact, a good balance between these two properties is critical for a good distribution in the organism by the bloodstream. The lipophilicity is directly related to the diffusion and permeation into the cellular lipid layer membrane, thus affecting not only to the activity of the drug, but also to its toxicity to healthy tissues. Moreover, lipophilicity is also related to plasma protein binding and metabolism of the drug.[23] Water solubility is also an important property, since it can influence on the absorption and distribution of the molecule. Mechanistically, although the precise target of gold species is still under debate, most of the investigations have unveiled that their cytotoxicity is due to their ability to alter mitochondrial functions through their binding to Se-containing enzymes like thioredoxin reductase (TrxR)[11, 24] and thioredoxin glutathione reductase; however, only a modest inhibitory effect is found on glutathione reductase.[25, 26] Thioredoxin reductase (TrxR) is an important and ubiquitous enzyme critically involved in the regulation of intracellular metabolism. Besides, the thioredoxin/thioredoxin reductase system plays a crucial role in the defense against oxidative damage and thus, in redox signaling. The interaction between gold-based organometallic drug and TrxR seems to lead to inhibition of the enzyme. As a result, there is an increase of the reactive oxygen species (ROS) and consequently, cell death via apoptosis.[25, 27] TrxR system is an excellent target because it is overexpressed in tumor cells,[28, 29] which implies more tendency of the gold drugs to these kind of cells and therefore, more selectivity than other organometallic complexes. In previous works, we have reported that the use of water soluble phosphanes of the type 1,3,5-triaza-7-phosphaadamantane (PTA), has led to water soluble gold(I) derivatives with antitumor properties against ovarian and/or colon cancer cells.[15, 16, 18, 19, 30] In this study, we report the tailored design of a new family of phosphanegold(I) thiolate with another even more water soluble phosphane, hexamethyl phosphorous triamide (HMPT). In addition, the gold(I) center is coordinated to different aromatic thiolate ligands, which have been selected due to their solubility and their demonstrated antiproliferative activity in other gold derivatives.

Results and discussion

Synthesis and characterization

The conventional route for the synthesis of thiolate gold(I)derivatives consists of the addition of [AuCl(HMPT)] (1) to a solution of the thiol in the presence of a base. All the obtained complexes are air stable solids with the formula [Au(SR)(HMPT)] (SR: Spy **2**, Spyrim **3**, SMe_2pyrim **4**, Sbenzothiazole **5**, Sthiazoline **6**, Sbenzimidazole **7** and 2-thiouracil **8**) (**Scheme 1**) in good yields.

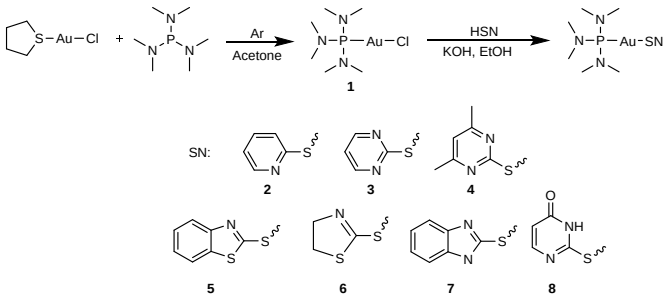

Scheme 1. Preparation of gold(I) derivatives with HMPT.

The coordination of the SR ligand can be confirmed by IR spectroscopy, thanks to the Au–Cl stretching vibration. This band is clearly visible in the complex **1** spectrum at 320 cm^{-1}, but it disappears after the reaction with the thiolate in all cases. Besides, aromatic bands are also appreciable, although the different rings of the thiol group are better characterized by ^{1}H NMR. In addition of the ring signals, all of them show the characteristic signal of the HMPT phosphane, a doublet signal of the 18 protons in their ^{1}H NMR spectra. The $^{31}P\{^1H\}$ NMR displays a low-field displaced singlet compared to those in the free phosphane, but at higher field respect to the starting material [AuCl(HMPT)] (**1**) as a consequence of the coordination to the SR ligand (**Table 1**).

Table 1. ^{31}P {^{1}H} NMR shifts for [Au(SR)HMPT] complexes.

$^{31}P\{H\}$NMR	1	2	3	4	5	6	7	8
δ(ppm)	110.87	124.05	124.05	124.43	121.06	122.8	120.78	120.88

Crystallographic Studies

Suitable crystals for X-ray structure determination were grown from complexes **4**, **5** and **8**. The structures reveal the typical linear two-coordinated geometry of the Au(I) cation with the angles S-Au-P being 173.35(5)° and 178.03(4)° respectively. The crystal group and system are different for each complex, whereas complex **4** crystallizes in *P*-1 triclinic group, complex **5** does in

$P2_1/c$ monoclinic group. The length of Au-P distances in complex **1** is 2.222(3) Å,[31] the same bond Au-P in complexes **4** and **5** shows very similar lengths, 2.2623(13) and 2.2643(11) Å, as there is no additional steric effects or repulsion to take into account. Besides, although the Au···Au distance for complex **5** is longer than for complex **4**, 6.635 (for **4**) and 9.397 (for **5**) Å, in both cases these distances are larger than the sum of vdW radii, so there is no aurophilic interaction between metal centers (**Figure 2**).

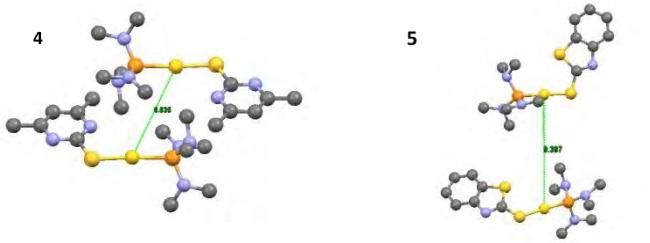

Figure 2. X-Ray structures for complexes **4** and **5**. Au···Au distances are represented in green.

Crystal of complex **8** was grown and measured by X-Ray diffraction. Although the data of this crystal structure high quality, they are good enough to allow a preliminary study of the complex. This study permits to observe intermolecular H-bonds between a NH unit from one 2-thiouracile molecule and the oxygen of the carbonyl group from other neighbor ligand. Au···Au distance is 5.375 Å so, and no metal interaction is observed (**Figure 3**).

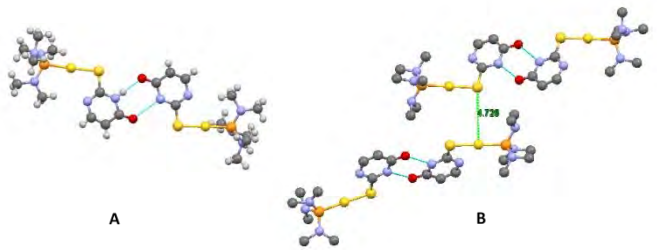

Figure 3. A. H bonds observed for complex **8**. **B**. Au-Au distances are represented in green.

The intermolecular interactions of these three complexes are very different. Complex **4** presents a strong stacking interaction between the aromatic rings (3.357 Å), which generates a bimolecular entity (**Figure S2**). Nevertheless, complex **5** does not establish this kind of interactions, so no different molecules are stacked in bigger units. It is worth to be mentioned the case of complex **8** where a double and stronger interaction can be observed. This interaction is provoked by the hydrogen bond between N6 and O3 atoms, and on the other hand N11 and O2 atoms (**Figure S3**), with distances of 2.839 and 2.754 respectively. These double interactions contribute to the stabilization of bimolecular entities in the crystalline structure.

Lipophilicity

View Article Online
DOI: 10.1039/C9DT04423J

It is necessary for a drug to have certain ADMET-tox properties, being some of them water solubility, lipophilicity, permeability or stability. The first two are very important but what is more crucial is the balance between them. It is known that membrane cell is composed of lipids, in contrast to the intracellular medium which is aqueous, so to get a good biodistribution, a drug has to possess both properties balanced (lipophilicity and hydrophilicity). To study these two properties, firstly water solubility measures were performed (**Table 2**). Despite the carefully structural design of our complexes with the presence of a water soluble phosphane and a lipophilic thiol, they seem not be so water soluble as we expected. In fact, they are less soluble than complex **1**, which is coherent with the larger size of the thiol group compare to the chlorine atom. Nevertheless, as it was mentioned before, water solubility is not determinant, but it is the balance of hydro- and lipophilicity. This characteristic can be measured by partition coefficient water/octanol, log P (for neutral complexes). In this work, we used the shake-flask method [32] to study the distribution of our complexes in aqueous and n-octanol media. The physicochemical similarity of 1-octanol to lipids makes it the most appropriate hydrophobic solvent. High values of lipophilicity of gold(I) complexes usually implies high toxicity because the drug is accumulated in the mitochondria [33, 34]. This is why a correct design of the drug is needed and the incorporation of hydrophilic moieties in the complexes is more and more common. The ideal ranges of lipophilicity for orally administrated drugs have been indicated to be $0 \leq \log P \leq 3$, so according to the experimental data obtained (**Table 2**), all gold(I) complexes show good values of $LogP_{7.4}$, and could be considered potentially oral drugs.

Table 2. Distribution coefficients of complexes **1**-**8**.

	Cis-Pt	Auranofin	**1**	**2**	**3**	**4**	**5**	**6**	**7**
Water Solubility (mg/L)	1.2[35]		460	103	180	220	140	300	189
Log $P_{7.4}$	-0.53[20]	2.53[35]	0.76	0.93	1.02	1.10	0.98	0.74	0.89

As it can be observed, the more H-bond donor atoms are in the molecule, the closer to zero are the $LogP_{7.4}$ values, which is normal because these atoms increase the probability of water solubility. Besides, the size of the thiol residue is something to take into account, because water solubility is easier for small molecules. These factors are consequent with the fact that complex **8** presents the least value for this property. On the other hand, we studied the impact of the both units of the complex, phosphane and thiol group, in order to establish the better phosphane moiety or thiol ligand to use, being this fact a crucial step in the correct design of a drug. Based on the **Table 3** it may be inferred that the use of HMPT is positive to achieve a balanced Log $P_{7.4}$. In contrast, the ionic character of the $[PTA\text{-}R]^+$ derivatives makes the gold(I) complexes too water soluble, with the exception of the PTA-CH_2-*p*-(NO_2-Ph) phosphane.

View Article Online
DOI: 10.1039/C9DT04423J

Table 3. Evaluation of the impact of phosphane (HMPT, this work and $[PTA-R]^+$ Ref. 14, 15) and thiol unit on the Log $P_{7.4}$ values of gold(I) complexes in Caco-2/TC7 cell line.

Phosphane			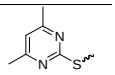
	Log $P_{7.4}$		
HMPT	0.93	1.02	1.10
PTA-CH_2Ph	0.15	0.18	-0.48
PTA-CH_2COOMe	-0.30	-0.26	-0.46
PTA-CH_2-*p*-(COOH-Ph)	-0.44	-0.83	-0.81
PTA-CH_2-*p*-(CH_2COOH-Ph)	-0.35	-0.88	-0.79
PTA-CH_2-*p*-(NO_2-Ph)	1.03	1.24	1.20

Solution Stability Studies.

Based on the distribution coefficient values of our complexes, a proper uptake can be assumed, but once the complex reaches the intracellular medium, several processes may be held. The intracellular medium is plenty of biomolecules which gold(I) center may interact with and thus, the complex may change its structure due to hydrolysis or redox reactions. Therefore, stability of the complexes has to be evaluated as another important pharmacokinetic property. Firstly, due to the poor water solubility observed, a previous solution in DMSO was required to perform the stability test. Each gold complex was dissolved in DMSO ($6{\cdot}10^{-3}$ M) and then diluted in the corresponding working solvent at pH 7.4, to a final concentration of $5{\cdot}10^{-5}$ M. The solution stability of the complexes was analyzed by absorption UV–vis spectrophotometry over 24 h at 37 °C, in order to simulate physiological conditions. The first test was carried out in PBS buffer solution and no reduction processes were observed, whereas no new bands over 580 nm appear. These results are hopeful because the gold toxicity is usually due to the accumulation of gold(0). In several complexes, a slightly decrease of the intensity can be appreciated especially at 24 hours, which may point hydrolysis processes. Moving to a more complex environment, we worked in a solution of PBS with 20% (*v*/*v*) complete medium (Supplemented Dulbecco's Modified Eagles medium (DMEM) see Experimental Section). This medium was selected because it is the cell culture medium, and it is important to test the stability in this medium in order to determine possible prodrug behavior. In the UV-vis spectra, a hyperchromic effect was observed in the 300 nm band (**Figure 4**), which is usually associated with the formation of Au-O bonds, something that could point hydrolysis processes.[36] In contrast to the results in PBS buffer, in the presence of DMEM, reactions of reduction were observed for complex **7**.

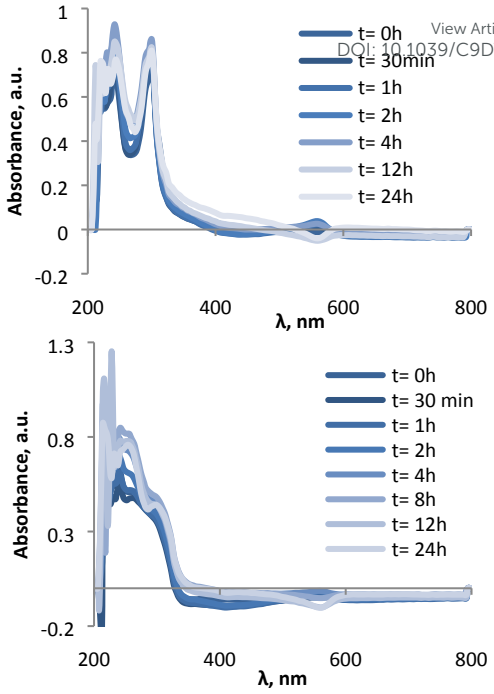

Figure 4. UV-vis spectra of complex **7** (up) and **8** (down) in PBS with 20% (*v*/*v*) complete medium.

Bovine Serum Albumin Interaction.

Most chemotherapeutic complexes benefit proteins present in bloodstream to achieve its target. Several are the proteins in plasma, but there is one more significant than the others, the human serum albumin (HSA); not only because of its major concentration (500-750 μM), but also because of its role in drug delivery.[37] Thus, the interaction between albumin and the drug may determine the drug's uptake and distribution. For this reason, the study of albumin binding is an important part to evaluate included in the mentioned ADME-tox properties. Its structure has been determined by X-ray diffraction and has been fully characterized. However, it is more frequent the use of the bovine serum albumin (BSA), as it is similar to HSA, with a homology of ca. 76%, and commercially available. The structure of BSA has also been determined by X-ray diffraction and it is fully characterized. It contains 585 amino acids and two main binding sites I and II,[38] where substances can be bound. The strength of this interaction should be studied in order to evaluate if it is strong enough for transport but also weak to deliver the drug once the target is reached. In addition, BSA presents an intrinsic fluorescence, mainly due to two tryptophan residues: Trp134, found on the surface of the protein, and Trp212, located in a hydrophobic binding pocket.[39] Most of the drugs are well biodistributed and delivered thanks to its binding to plasmatic proteins. This bond usually implies changes in many properties of the drug. To study the binding between the albumin and the compounds several techniques could be used, but in order to study albumin binding of gold complexes, fluorescence and UV-Vis spectroscopy are the most commonly used. A low protein binding seems to be

advantageous, since some authors have indicated a high affinity for protein thiols restricts the *in vivo* anticancer activity of gold(I) complexes compared to its *in vitro* activity.[40] In other words, a strong binding to albumin can limit the distribution of the drug thus limiting its effectiveness. In order to study the affinity of some of the new complexes synthesized for albumin, we have carried out some spectroscopic experiments of fluorescence. The intrinsic fluorescence of BSA is very sensitive to the environment, so a weak interaction with some molecules can produce changes in their emission spectrum. In this study we observed that the addition of increasing amounts of thiolate derivatives to a solution of BSA resulted in a quenching of its fluorescence emission upon excitation at 295 nm. The fluorescence data have been analyzed using the Stern-Volmer equation to quantify the strength of the binding between gold complex and BSA. To do this, it is necessary to plot F_0/F versus [complex] (F_0 = intensity in the absence of the quencher; F = intensity in the presence of the quencher), as it can be seen in the figure below.

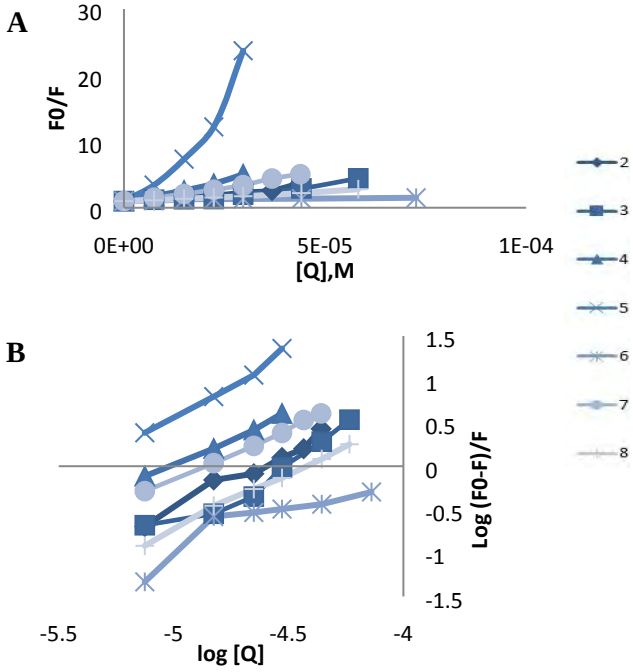

Figure 5. Stern–Volmer (**A**) and Modified Stern-Volmer (**B**) plots for the quenching of BSA with increasing amounts of gold(I) complexes (complex concentration from 0 to 170 (**1**), 43.8 (**2** and **7**) 58.3 (**2** and **8**), 29.6 (**4** and **5**) and 72.6 (**6**) μM) at 298 K (λexc = 295 nm, [BSA] = 50 μM).

The determination of the operated quenching of fluorescence gives useful information because while static quenching implies the formation of ground-state complex, in dynamic quenching only are diffusion processes.[41] kq parameter is especially important in this study, the value of this constant indicates which type of quenching operates. Due to dynamic quenching depends on diffusion, a kq value higher than the diffusion controlled rate constant of the biomolecule in water, 10^{10} M^{-1} s^{-1}, could indicate some type of binding interaction, implying a possible contribution of static quenching. In our case, the values of kq are in the order of $10^{11\text{-}13}$ M^{-1} s^{-1}, so binding of the complexes and BSA could be considered (**Table 3**). Previously, it was mentioned that BSA contains different domains where drugs can bind, and thus more than one drug can be linked to the BSA. Stern-Volmer modified equation permits calculate the values of the binding constant (Kb) for each experiment and the number of binding sites (n) (**Table 4**). According with the results, there is only one gold molecule coordinated to BSA, and this bond is in agreement with those observed for other gold(I) derivatives,[14, 17] but slightly larger than the binding constant of *cis*platin.[42] As it can be seen in **Table 4**, complex **1** presents a lower *n* value than the rest of the derivatives, so the substitution of the chloride atom for the thiol group is positive in order to achieve a better interaction between our complexes and BSA. Complex **1** seems to interact only with the half of the BSA molecules.

Table 4. Values of the Stern–Volmer quenching constant (K_{SV}), bimolecular quenching constant (Kq), number of binding sites (n) and binding constant (Kb) for the interaction of gold(I) complexes with BSA.

Complex	K_{sv} (M^{-1})	K_q (M^{-1} s^{-1})	K_b (M^{-1})	n
1	$1.12 \cdot 10^3$	$1.12 \cdot 10^{11}$	$0.59 \cdot 10^2$	0.58 (1)
2	$4.95 \cdot 10^2$	$4.95 \cdot 10^{12}$	$1.51 \cdot 10^6$	1.33 (1)
3	$4.66 \cdot 10^2$	$4.66 \cdot 10^{12}$	$2.83 \cdot 10^6$	1.43 (1)
4	$1.25 \cdot 10^5$	$1.25 \cdot 10^{13}$	$9.43 \cdot 10^5$	1.19 (1)
5	$6.25 \cdot 10^5$	$6.25 \cdot 10^{13}$	$2.57 \cdot 10^8$	1.57 (2)
6	$8.24 \cdot 10^3$	$8.24 \cdot 10^{11}$	$4.57 \cdot 10^3$	0.93 (1)
7	$8.78 \cdot 10^2$	$8.78 \cdot 10^{12}$	$5.35 \cdot 10^5$	1.18 (1)
8	$2.83 \cdot 10^3$	$2.83 \cdot 10^{12}$	$4.65 \cdot 10^5$	1.28 (1)

Cytotoxicity assays

All complexes synthesized were tested against different tumor cell lines: A2780, A2780R (ovarian cancer) and Caco2/TC7 (human colon adenocarcinoma). The IC_{50} values (**Table 5**) were calculated by using the MTT viability assay.[43]

Table 5. IC_{50} values (μM) of gold(I) complexes in A2780 and A2780R cells (HMPT, this work and PTA Ref. 18, 19).

	1	2	3	4	5	6	7	8
				A2780				
HMPT	0.86±0.01	0.76±0.01	0.70±0.01	0.26±0.01	0.7 ±0.01	0.47±0.02	0.99±0.02	0.41±0.03
PTA		9.6 ±2.3	5.7±1.9	0.7±0.1	0.8±0.2	0.7±0.3	8.0±0.6	
				A2780R				
HMPT	2.70±0.01	1.27±0.02	1.44±0.02	0.64±0.01	2.12±0.02	0.94±0.01	2.34±0.02	0.93±0.01
PTA		8.2 ±2.8	4.1±2.5	0.8±0.5	0.9±0.1	1.1±0.1	23.9±2.51	

The results are expressed as mean values ± log SEM *(n ≥ 12 experiments).*

Previous studies with different phosphane groups were done in our research group and allowed us to compare the cytotoxic influence of the phosphane. In this case, we can deduce that in A2780 and A2780R cell lines, the use of the phosphane HMPT enhances the antiproliferative activity compared to the observed with PTA. Besides, all of our complexes are strongly better than *cis*-platin in both cell lines (4.30±0.5 for A2780 and 18.2±0.5 for A2780R).[18]

In addition to this study, gold(I) derivatives were also tested on colon cancer Caco-2/TC7 cell line.[44, 45] This cell line implies an extra advantage for our antitumor research, because once cells reach the state of differentiation, they acquire morphological properties of normal epithelial cells which allow us to evaluate the selectivity of all gold(I) complexes.[44, 46] For this purpose, cytotoxicity experiments were carried out in cancer cells (5 days after seeding) and in normal cells (5 days after seeding). Remarkably, as it can be seen in **Table 6**, complexes **7** and **8** do not show any effect on normal cells even at concentrations 5 fold higher than the IC_{50} values obtained in cancer cells. For this reason, these two compounds are excellent candidates to perform additional studies about its action mechanisms. However, complexes **2-6** were no longer considered as candidates for antitumour application, as they reduced the viability of normal cells.

Our studies carried out in the Caco-2 cell line also show the great cytotoxic effect of all our complexes based on IC_{50} values in cancer cells. Although our complexes are not so active as auranofin (2.1±0.40 μM), they are better than *cis*-platin (45.6±8.08),[47] not only due to their antiproliferative activity but also their selectivity.

Table 6. IC_{50} values (μM) of gold(I) complexes in Caco2/TC7 cells.

View Article Online DOI: 10.1039/C9DT04423J

IC_{50}	2	3	4	5	6	7	8
Cancer cells	3.87±0.15	3.08±0.14	3.17±0.10	3.16±0.20	7.40±0.10	4.50±0.10	4.55±0.11
Normal cells	10.5±0.07	5.14±0.08	8.81±0.09	11.3±0.08	10.1±0.14	>>20	>>20

The results are expressed as mean values ± log SEM (n ≥ 12 experiments).

Based on the different activity observed for the phosphane in coordination to gold center in the ovarian cell line A2780, a similar study was performed with the Caco-2/TC7 cell line (**Table 7**). These results point to the high impact of the phosphane group in antiproliferative activity. In fact, IC_{50} values can vary from 2.68±0.30 with the PTA-CH_2-*p*-(COOH-Ph) to 7.67±1.50 with the unit PTA-CH_2COOMe.

Table 7. Evaluation of the impact of phosphane and thiol unit on the IC_{50} values (μM) of gold(I) complexes in Caco-2/TC7 cell line (cancer cells). (HMPT, this work and $[PTA\text{-}R]^+$ Ref. 14, 15)

Phosphane	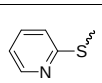		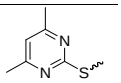
	IC_{50} (μM)		
HMPT	3.87±0.15	3.08±0.14	3.17±0.10
PTA-CH_2Ph	5.05±0.05	3.95±0.04	7.50±1.5
PTA-CH_2COOMe	7.67±1.50	2.80±1.0	6.37±1.3
PTA-CH_2-*p*-(COOH-Ph)	2.68±0.30	6.47±2.15	7.66±0.09
PTA-CH_2-*p*-(CH_2COOH-Ph)	4.61±0.14	10.66±2.56	6.29±1.07
PTA-CH_2-*p*-(NO_2-Ph)	3.08±0.79	2.98±1.28	3.96±1.33

The results are expressed as mean values ± log SEM (n ≥ 12 experiments).

Effects on Reactive Oxygen Species (ROS) generation.

Interaction with TrxR Systems. Thioredoxin system has been generally considered one of the main targets of gold compounds. This system participates in the control of redox equilibrium of the cell by removing the excess of oxidant species. One of the reasons why Trx system is an appropriated target relies in its overexpression in some cancer cells in tumours, related to aggressive tumour growth and inhibition of apoptosis.[29] Besides, the presence of cysteine and selenocysteine residues in the enzyme makes possible the binding with soft metals as gold(I). It is believed that the coordination of gold(I) and other metals to the TrxR results in its inhibition. The breaking of the equilibrium between oxidant and antioxidant species promotes the oxidative stress in the cell, leading to apoptosis processes.[48, 49] We studied the inhibition of the thioredoxin reductase in Caco-2/TC7 cell lysates, in contrast with other investigations, in which isolated TrxR protein from rat liver is used.[50, 51] A strong decrease of the

View Article Online
DOI: 10.1039/C9DT04423J

TrxR activity was observed for complexes **7** and **8** compared with the basal activity registered for the control lysate (**Figure 6**). The coordination of the gold(I) phosphane complexes seems to be selective to TrxR system comparing to the observed affinity to other similar enzyme as glutathione reductase.[52]

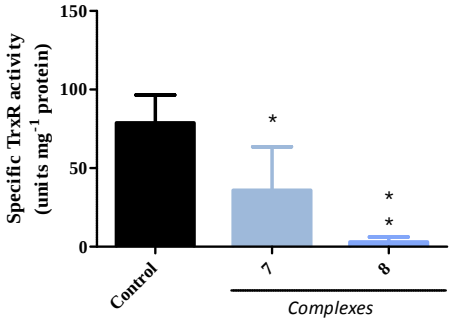

Figure 6. Specific TrxR activity (units/ mg protein) in Caco-2/TC7 cells with complexes **7** and **8** (20 µM, 24 h). *P<0.05; **P<0.01 vs. control (n ≥ 4 experiments).

Stress Oxidative Damage. Based on the above results, we hypothesized that stress oxidative might be enhanced and consequently, damage on different biomolecules such as proteins and lipids might be present. So in the next step of the current investigation, we measure the products of proteins and lipids oxidation. ***Protein oxidation evaluation.*** Oxidation processes in proteins can give different products and thus, there are diverse methods to evaluate the damage on proteins, but the most established one is the quantification of carbonyl species.[53] . Although proteins are very sensitive biomolecules, no evidence of oxidative damage was observed with the two gold(I) complexes used (**Figure 7A**). ***Lipid peroxidation evaluation*.** Lipids present in the membrane layer can also be easily oxidized to form peroxidised species such as malondialdehyde (MDA) or hydroxyalkenals (4-HDA), which are important biomarkers to evaluate lipid oxidative damage. In order to measure both biomarkers at the same time, we use Gerard-Monier method.[54] In contrast with the observed in protein oxidation assay, now we found a significant increase in the MDA + 4-HDA levels after the treatment with complexes **7** and **8** respect to the DMSO-control (**Figure 7B**). These differences permit conclude that our complexes promote an oxidative damage in lipids of the cell membrane. Other studies point that the inhibition of the TrxR systems usually provokes the formation of hydrogen peroxide.[24] This increase of hydrogen peroxide may trigger a signalling event of controlled cell death but, according to concentration and site of production, it may also provoke an irreversible oxidative stress damage.[55]

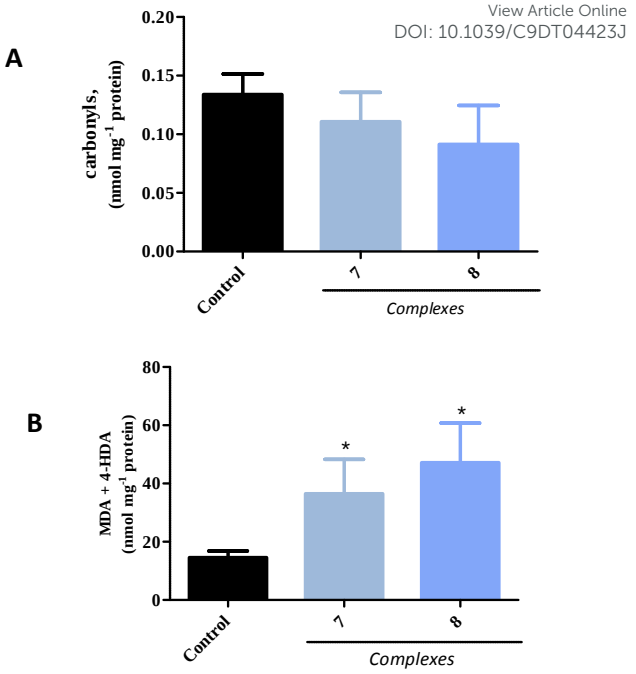

Figure 7. (**A**) Carbonyl species levels (**B**) MDA+4-HDA levels (nmol mg^{-1} protein) in Caco-2/TC7 cells with complexes **7** and **8** (24 h, 20 µM). *P<0.05 vs. control. (n≥ 6 experiments)

Apoptosis studies in cancer cells. We thought that maybe this oxidative damage in the membrane lipids, as a consequence of the inhibition of the thioredoxin reductase enzyme, might promote apoptosis processes. Drugs can trigger different mechanisms of cell death, but apoptosis is the pathway responsible for the cell proliferation control; a hundred thousand cells are produced every second by mitosis processes, while an equivalent number of cells is destroyed by apoptotic processes.[56] Consequently, several apoptosis assays were performed with the selective complexes **7** and **8**. Firstly, we studied the ability of our compounds to induce apoptosis by flow cytometry, by using a combination of the markers 7-Aminoactinomycin D (7-AAD) and annexin V-FITC. In apoptotic cells, the exposure of phosphatidylserine (PS) usually occurs prior to the loss of plasma membrane integrity,[57, 58] so external PS can be defined as a marker of apoptosis.[57, 59] Due to the selective reaction of PS with annexin, healthy cells will be unreactive. As it can be seen in **Figure 8B**, both gold(I) complexes exhibit a slightly increase in population of cells undergoing apoptosis (in early and late stages) compared to control, although this increase was not statistically significant. Only a negligible percentage of necrotic cells was observed.

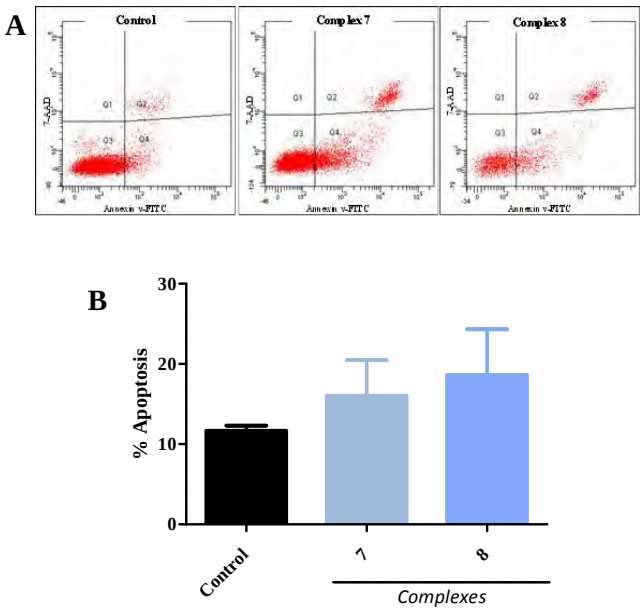

Figure 8. (**A**) Fluorescence histograms of the distribution of cell populations in different stages: necrosis (Q1), living cells (Q3), late apoptosis (Q2) and early apoptosis (Q4), in control and gold(I) complexes treated Caco-2/TC7 cells. (**B**) Apoptosis values, early + late, (%) of cells treated with gold(I) complexes (20 µM, 24 h). The results are expressed as mean ± SEM (n ≥ 4 experiments).

Cell cycle Studies. The mutations responsible for the formation and growing of tumour are significantly controlled by the cell cycle. In fact, cancer cells usually imply changes in the normal performance of the cell cycle, and therefore studies of the cell cycle of Caco-2/TC7 by using flow cytometry were carried out (**Figure 9**). The cell populations obtained in the histograms show that most of cells are found in the G0/G1 phases, which is something normal, as cells spend the most part of their lives in these phases.[60, 61] Comparing the values of the cells in the different stages of the cycle, no significant increase of the number of cells in S or G2/M phase was shown by complex **7** and **8**. These results suggest that complexes **7** and **8** might not alter the cell cycle in its action mechanisms (**Table 8**). This fact was also observed with other different gold(I) complexes with no impact on the antiproliferative activity.[62]

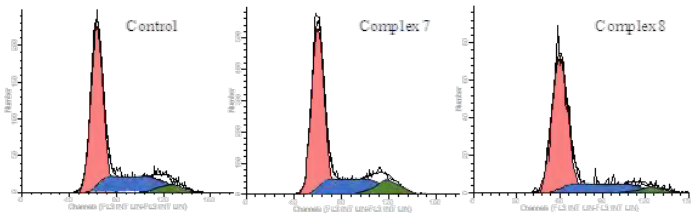

Figure 9. Fluorescence histograms obtained by flow cytometry of the cell populations in different phases of the cell cycle after 24 h of incubation of the cells with DMSO (control) and gold(I) complexes **7** and **8** (20 µM).

Table 8. Cell populations (%) in the different phases of the cell cycle for complexes **7** and **8** (20 µM, 24 h).

	G0/G1	S	G2/M
Control	60.25±1.53	33.02±1.25	6.73±0.55
7	59.51±4.42	34.67±4.39	5.05±0.49
8	60.89±4.23	30.63±3.50	8.48±1.22

*Values are expressed as mean ± EEM (n ≥ 4 experiments). *P<0.05; **P<0.01 vs. control.*

Apoptosis studies in primary cultures of mouse colon tumours. Once *in vitro* assays were performed, as the obtained apoptosis results were inconclusive, we decided to test our compounds in primary cultures of colon tumours from mice. This model allows us to test our complexes in conditions more similar to what happens in colon cancer. In this experimental model we employed dextran sodium sulfate (DSS) to induce epithelial damage in combination with azoxymethane (AOM), a potent carcinogenic that can produce colonic tumorigenesis in over a period of 10 weeks.[63, 64] The isolated tumor tissue was subjected to enzymatic digestion to obtain individual cancer cells. Then, the same protocol as in the *in vitro* model of cells was carried out to detect the exposure to phosphatidylserine. Surprisingly, working in a more real tumor model, the result was different in contrast to the *in vitro* experiment (**Figure 10**); now complex **7** and **8** can be considered as proapoptotic drugs by PS signalizing apoptotic pathway.

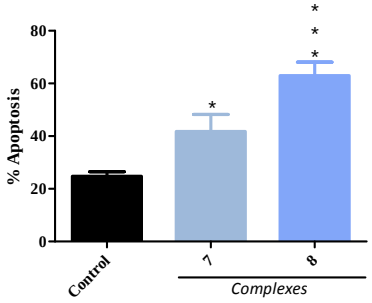

Figure 10. Apoptosis values, early + late, (%) of Caco-2 cells treated with gold(I) complexes (20 µM, 24 h). The results are expressed as mean ± SEM (n ≥ 4 experiments) *P<0.05; ***P<0.001 vs. control.

EXPERIMENTAL SECTION

General procedures

NMR Spectroscopy. ^{1}H, ^{31}P and ^{13}C NMR spectra were recorded on 400 or 300 MHz Bruker Avance spectrometers and are referenced to external TMS or 85% H_3PO_4 (^{31}P), Chemical shifts (δ) are given in ppm, coupling constants are reported in Hz. MALDI mass spectra were measured on a Micromass Autospec spectrometer in positive ion mode using DCTB (1,1-diciano-4-^{t}butylphenyl-3-methylbutadiene) as matrix. Infrared spectra (4000-250 cm^{-1}) were recorded on a Perkin Elmer Spectrum 100 FTIR (far-IR)

spectrometer. Elemental analyses were obtained in-house using a LECO CHNS-932 microanalyser. The starting material: the phosphane HMPT was purchased from Alfa Aesar (Kandel, Germany) and the thiols were purchased from Sigma-Aldrich (Madrid, Spain) and used as received. [AuCl(tht)] was prepared according to published methods,[65] and [AuCl(HMPT)] with a slightly modified procedure.[31]

WARNING: Special care must be taken with the phosphane, thus working in a well-ventilated place is extremely recommended.

Synthesis and Characterization.

[AuCl(HMPT)] (1). To a suspension of [AuCl(tht)] (2 mmol, 0.643 g) in 20 mL of acetone in a shlenk tube under argon was added 3 mmol of HMPT (2 mmol, 0.489 g, 0.365 mL) and stirred for 1 h at room temperature. The resulting solution was evaporated until dryness and a white solid is observed. Yield: 93% white solid. ^{1}H NMR (400 MHz, $CDCl_3$) δ (ppm) 2.66 (d, J_{H-P} = 11.7 Hz, 18H). ^{31}P {^{1}H} NMR (162 MHz, $CDCl_3$) δ(ppm) 110.87 (s). APT-RMN (101 MHz, $CDCl_3$) δ(ppm) 37.79 (d, J_{C-P}=9.2 Hz) IR (ν(cm^{-1})): 2922, 1462, 1425, 1408, 1281, 1179, 1149, 1063, 958, 719, 677, 523, 316. MS (MALDI$^+$, m/z (%)):270.2 (58.8, [Au-PNMe$_2$]$^+$), 360.1 (46.2, [M-Cl]$^+$), 523.2 (100, [M-Cl+HMPT]$^+$), 755.1 (22.1, [2M-Cl]$^+$). $S_{25ºC}$ H_2O (mg/L)= 496.6

Preparation of the complexes (2)-(8). To an ethanolic solution (20 mL) of 2-mercaptopyridine (**2**), 2-mercaptopyrimidine (**3**), 4,6-dimethyl-2-mercaptopyrimidine (**4**), 2-mercaptobenzothiazole (**5**), 2-mercaptothiazoline (**6**), 2-mercaptobenzimidazole (**7**) and 2-thiouracil (**8**) (0.3 mmol); was added a solution of KOH in ethanol (0.33 mmol). After 30 min of stirring, [AuClHMPT] (0.3 mmol, 0.119 g) was added, and the mixture was stirred for 24 h at room temperature, and the KCl was filtered off. The colourless solution was then, evaporated until 5 mL and filtered the formed solid.

[Au(2-Spy)HMPT] **(2).** Yield: 99% yellow solid. ^{1}H-NMR (400 MHz, $CDCl_3$): δ (ppm) 8.16 (ddd, *J*= 5.0, 1.9, 0.8 Hz, 1H, Hpy-H6), 7.44 (d, *J*=8.0 Hz, 1H, Hpy-H3), 7.26-7.20 (m, 1H, Hpy-H4), 6.77 (ddd, *J*=7.3, 5.0, 1.1 Hz, 1H, Hpy-H5), 2.65 (dd, J_{H-P}=11.6 Hz, 3.2 Hz, 18H, HMe) APT (100.62 MHz, $CDCl_3$): δ (ppm) 128.83, 126.65, 118.07 (Cpy-C5), 37.86 (d, J_{C-P} =9.5Hz, CMe). ^{31}P{^{1}H}-NMR (162 MHz, $CDCl_3$): δ (ppm) 124.05 IR (ν (cm^{-1})): 2879, 1563, 1535, 1445, 1407, 1370, 1282, 950, 716, 677, 631, 519. MS (MALDI$^+$) m/z (%): 523.2 (47.0, [AuHMPT+HMPT]$^+$), 830.1 (100, [M+AuHMPT]$^+$), 1137.1 (3.6, [2M+Au]$^+$). Anal. Calc. for $C_{11}H_{22}AuN_4PS$: C, 28.09; H, 4.71; N, 11.91; S, 6.82. Found: C, 28.22; H, 4.33; N, 11.77; S, 6.47%.

[Au(2-Spym)HMPT] **(3).** Yield: 98% pale yellow solid. ^{1}H-NMR (400 MHz, $CDCl_3$): δ (ppm) 8.27 (d, *J*=4.8Hz, 2H, Hpy-H4), 6.76 (t, *J*=4.8Hz, 1H, Hpy-H5), 2.71 (d, J_{H-P}=11.5 Hz, 18H, HMe) APT (100.62 MHz, $CDCl_3$): δ (ppm) 156.56 (Cpy-C4), 115.40 (Cpy-C5), 37.87 (d, J_{C-P} =9.6Hz, CMe) ^{31}P{^{1}H}-NMR (162 MHz, $CDCl_3$): δ (ppm) 124.05 IR (ν (cm^{-1})): 2918, 1561, 1535, 1369, 1283, 1186, 1169, 1063, 948, 774, 740, 711, 678, 518. MS (MALDI$^+$, m/z (%)): 523.2 (9.9, [AuHMPT+HMPT]+), 831.1 (100, [M+AuHMPT]$^+$), 1139.2 (3.7, [2M+Au]$^+$). Anal. Calc. for $C_{10}H_{21}AuN_5PS$: C, 25.48; H, 4.49; N, 14.86; S, 6.80. Found: C, 25.59; H, 4.44; N, 15.12; S, 7.01%.

[Au(4,6-dimethyl-2-Spym)HMPT] **(4).** Yield: 94% pale yellow solid ^{1}H-NMR (400 MHz, $CDCl_3$): δ (ppm) 6.76 (s, 1H, Hpy-H3), 2.66 (d, *J*= 11.7 Hz, 18H, HMe), 2.40 (d, J_{H-P}=11.5 Hz, 6H, Hpy-HMe). APT (100.62 MHz, $CDCl_3$): δ (ppm) 165.89 (Cpy-C3), 114.49 (Cpy-C4), 37.90 (d, J_{C-P}=9.7 Hz, CMe), 23.93 (Cpy-CMe). ^{31}P{^{1}H}-NMR (162 MHz, $CDCl_3$): δ (ppm) 124.43. IR (ν (cm^{-1})): 2895, 1619, 1573, 1540, 1288, 1246, 971, 948, 719, 679, 520. MS (MALDI$^+$) m/z (%): 523.2 (4.6, [AuHMPT+HMPT]$^+$), 859.1 (100, [M+AuHMPT]$^+$), 1195.1 (7.4, [2M+Au]$^+$). Anal. Calc. for $C_{12}H_{25}AuN_5PS$: C, 28.86; H, 5.05; N, 14.02; S, 6.42. Found: C, 28.99; H, 5.14; N, 14.25; S, 6.35%.

[Au(2-Sbenzothiazole)HMPT] **(5).** Yield: 97% white solid. ^{1}H-NMR (400 MHz, $CDCl_3$): δ (ppm) 7.69 (dd, *J*=8.1, 0.5 Hz, 1H, HPh-H7), 7.60-7.52 (m, 1H, HPh-H4), 7.33-7.26 (m, 1H, HPh-H6), 7.15 (ddd, *J*= 7.9, 7.4, 1.2 Hz, 1H, HPh-H5), 2.71 (d, J_{H-P}= 11.6 Hz, 18H, HMe). APT (100.62 MHz, DMSO): δ (ppm) 172.42, 155.96, 135.43, 125.56 (CPh-C6), 123.37 (CPh-C3), 120.51 (CPh-C4), 119.73 (CPh-C7), 37.17 (d, J_{C-P} =8.7Hz, CMe). ^{31}P{^{1}H}-NMR (162 MHz, $CDCl_3$): δ (ppm) 121.66. IR (ν (cm^{-1})): 3053, 2920, 2881, 1630, 1557, 1447,1413, 1281, 1182, 1059, 966, 720, 677, 520. MS (MALDI$^+$) m/z (%):523.2 (100, [AuHMPT+HMPT]$^+$), 886.1 (44.5, [M+AuHMPT]$^+$). Anal. Calc. for $C_{13}H_{22}AuN_4PS_2$: C, 29.66; H, 4.21; N, 10.64; S, 12.18. Found: C, 29.82; H, 4.25; N, 10.46; S, 12.39%.

[Au(2-Sthiazoline)HMPT] **(6).** Yield: 97% white solid. ^{1}H-NMR (400 MHz, $CDCl_3$): δ (ppm) 4.24 (t, *J*=7.9 Hz, 2H, Hthiazol-H5), 3.37 (t, *J*=7.9 Hz, 2H, Hthiazol-H4), 2.70 (d, J_{H-P}= 11.6 Hz, 18H, HMe). APT (100.62 MHz, DSMO): 65.62 (Cthiazol-C5), 37.83 (d, J_{C-P} =9.2 Hz, CMe), 36.47 (Cthiazol-C4). ^{31}P{^{1}H}-NMR (162 MHz, $CDCl_3$): 122.80. IR (ν (cm^{-1})): 3070, 2922, 2882, 1636, 1547, 1450, 1280, 1181, 1151, 962, 712, 670, 517. MS (MALDI$^+$) m/z (%): 523.0 (37.5, [AuHMPT+HMPT]$^+$), 837.8 (79.0, [M+AuHMPT]$^+$), 1111.8 (100, [M+AuHMPT+AuPN]$^+$). Anal. Calc. for $C_9H_{20}AuN_4PS_2$: C, 22.69; H, 4.23; N, 11.76; S, 13.36. Found: C, 22.85; H, 4.19; N, 11.89; S, 13.66%.

[Au(2-Sbenzimidazole)HMPT] **(7).** Yield: 89% white solid. ^{1}H-NMR (400 MHz, $CDCl_3$): δ (ppm) 7.37-7.31 (m, 2H, HPh-H4), 7.11-7.05 (m, 2H, HPh-H5), 2.71 (d, J_{H-P}= 11.6 Hz, 18H, HMe). APT (100.62 MHz, $CDCl_3$): δ (ppm) 121.28 (CPh-C4), 112.76 (CPh-C5), 37.85 (d, J_{C-P}=9.3 Hz, CMe). ^{31}P{^{1}H}-NMR (162 MHz, $CDCl_3$): δ (ppm) 120.78. IR (ν (cm^{-1})): 2881, 2835, 2791, 1425, 1270, 1184, 968, 717, 679, 520. MS (MALDI$^+$) m/z (%): 523.2 (27.4, [AuHMPT+HMPT]$^+$), 869.1 (39.1, [M+AuHMPT]$^+$), 1228.3 (100, [M+ 2AuHMPT]$^+$). Anal. Calc. for $C_{13}H_{23}AuN_5PS$: C, 30.65; H, 4.55; N, 13.75; S, 6.30. Found: C, 30.77; H, 4.61; N, 38.91; S, 6.61%.

[Au(2-thiouracile)HMPT] **(8).** Yield: 94% white solid. ^{1}H-NMR (400 MHz, $CDCl_3$): δ (ppm) 7.62 (d, *J*=6.7 Hz, 1H, Hthio-H5), 6.06 (d, *J*=6.7 Hz, 1H, Hthio-H4), 2.70 (d, J_{H-P}= 11.6 Hz, 18H, HMe). APT (100.62 MHz, DSMO): δ (ppm) 109.84, 37.79 (d, J_{C-P}= 9.2 Hz, CMe). ^{31}P{^{1}H}-

View Article Online DOI: 10.1039/C9DT04427J

NMR (162 MHz, $CDCl_3$): δ (ppm) 120.88. IR (ν (cm^{-1})): 3323, 3084, 2971, 2882, 1655, 1566, 1448, 1046, 968, 719, 677, 522. MS (MALDI$^+$) m/z (%): 523.2 (100, [AuHMPT+HMPT]$^+$), 847.2 (8.7, [M+AuHMPT]$^+$). Anal. Calc. for $C_{10}H_{21}AuN_5OPS$: C, 24.65; H, 4.34; N, 14.37; S, 6.58. Found: C, 24.79; H, 4.37; N, 14.58; S, 6.72%.

Single-Crystal Structure Determination. Suitable crystals of **4**, **5** and **8** were mounted on a glass fiber and used for data collection on a Bruker AXS APEX CCD area detector equipped with graphite monochromated Mo Kα radiation (λ = 0.71073 Å) by applying the ω-scan method. Lorentz-polarization and empirical absorption corrections were applied. The data reduction was performed with the APEX2 software (Bruker Apex2, Bruker AXS Inc., Madison, Wisconsin, USA, 2004) and corrected for absorption using SADABS (G.M. Sheldrick, SADABS, Program for Empirical Adsorption Correction, Institute for Inorganic Chemistry, University of Gottingen, Germany, 1996). Crystal structure was solved by direct methods and refined by full-matrix least-squares on F^2 including all reflections using anisotropic displacement parameters by means of the WINGX crystallographic package (G. M. Sheldrick, SHELX-2014, Program for Crystal Structure Refinement, University of Göttingen, Göttingen, Germany, 2014).[66] Generally, anisotropic temperature factors were assigned to all atoms except for hydrogen atoms, which are riding their parent atoms with an isotropic temperature factor arbitrarily chosen as 1.2 times that of the respective parent. Final R(F), wR(F^2) and goodness of fit agreement factors, details on the data collection and analysis can be found in Table S1. Selected bond lengths and angles are given in Table S2 (ESI). CCDC reference numbers for the structures of **4** and **5** were 1938214 and 1938215. The quality of the crystals in compound **8** was very low. Several samples have been measured and their structural properties have been studied. This cif file is included in the supporting information and has not been deposited in the CCDC. Copies of the data can be obtained free of charge upon application to CCDC, 12 Union Road, Cambridge CB2 1EZ, U.K. (fax, (+44)1223 336-033; e-mail, deposit@ ccdc.cam.ac.uk).

Cell culture. This study was carried out in the human enterocyte-like cell line Caco-2/TC7.[67] This cell line undergoes in culture a process of spontaneous differentiation that leads to the formation of a monolayer of cells, expressing morphological and functional characteristics of the mature enterocytes. This differentiation process is growth-dependent, where the cells undergo differentiation from 'undifferentiated proliferative crypt-type cells' in exponential phase of growth, to 'differentiated enterocyte-type cells' in stationary phase.[68] Caco-2/TC7 cells (passages 30-50) were cultured at 37ºC in an atmosphere of 5% CO_2 and maintained in high glucose DMEM supplemented with 2 mM glutamine, 100 U/mL penicillin, 100 µg/mL streptomycin, 1% non-essential amino acids, and 20% heat-inactivated fetal bovine serum (FBS) (Life Technologies, Carlsbad, CA, USA). To cell line maintenance, cells were passaged enzymatically with 0.25% trypsin-1 mM EDTA and sub-cultured on 25 cm^2 plastic flasks at a density of 10^4 cells/cm^2. Culture medium was replaced every 2 days. With this density of culture, the cells reach cell confluence 90% (where cell differentiation starts) at 7 days after seeding, and the complete cell differentiation is reached at 15 days post-seeding. Thus, experiments in undifferentiated and differentiated cells (considered as cancer and normal cells, respectively) were performed between 2-5 days and 12-15 days post-seeding, respectively. For cell viability assays, cells were seeded in 96-well plates at a density of 2 × 10^4 or 4 × 10^3 cells per well, and measurements were carried out 5 or 15 days after seeding, respectively. For thioredoxin reductase and oxidative stress assays, cells were seeded at a density of 3.3 × 10^4 cells/cm^2; and for apoptosis and cell cycle analyses at 3 × 10^4 cells/cm^2. Stock solutions of the complexes (in DMSO) were diluted in the complete medium to the required concentration. DMSO at similar concentrations did not show any cytotoxic effects. The culture medium was replaced with fresh medium (without FBS) containing the complexes at concentrations varying from 0 to 20 µM, and with an exposure time of 72 h for cell viability assays. For all the other studies, the cells were incubated at 20 µM for 24 h.

Cell viability assay. Cell survival was measured by using the MTT test.[43] The assay is dependent on the cellular reduction of 3-(4,5-dimethylthiazol-2-yl)-2,5-diphenyltetrazolium bromide (MTT, Sigma-Aldrich, Madrid, Spain) by the mitochondrial dehydrogenase of viable cells to a blue formazan product that can be measured spectrophotometrically. Following the appropriate incubation of cells, with or without the metallic complexes, MTT (5 mg mL^{-1}) was added to each well in an amount equal to 10 % of the culture volume. Cells were incubated with MTT at 37 °C for 3 h. After that, the medium and MTT were removed and 100 µl of DMSO was added to each well. The plate was gentle stirred in a shaker. Finally, the cell viability was determined by measuring the absorbance with a multi-well spectrophotometer (DTX 800 Multimode Detector, Beckman Coulter) at a wavelength of 560 nm and compared with the values of control cells incubated in the absence of the complexes. IC_{50} values were calculated using a conventional concentration-response curve with variable slope. Experiments were conducted in quadruplicate wells and repeated at least three times.

Apoptosis studies. For the studies of apoptosis, by means of the detection of phosphatidylserine in the outer layer of the plasma membrane, the Annexin V-FITC Apoptosis Detection kit (Immunostep, Spain) was used. After the incubation with the complexes, the cells were collected and transferred to flow-cytometry tubes. A negative control was prepared with untreated cells, that was used to define the basal level of apoptotic and necrotic or dead cells. The staining with Annexin V-FITC and 7-Aminoactinomycin D (7-ADD) was performed according to manufacturer's recommendation. The cells were washed twice with temperate phosphate-buffered saline (PBS) and resuspended in 200 µl of 1 x Annexin-binding buffer. Thereafter, 2.5 µl of the Annexin V-FITC and 2.5 µl of PI were added to each 50 µl of cell suspension. After incubation for 15 min at RT in the dark, 400 µl of

1 x Annexin binding buffer were added and analyzed by flow cytometry within 1 h. The signal intensity was measured using a Gallios Flow Cytometry (Beckman Coulter) and analyzed using the Kaluza Analysis Software (Beckman Coulter).

Cell cycle analyses. After the incubation with the complexes, the cells were collected, washed twice with PBS, fixed in 70% ice-cold ethanol and stored at 4 °C for 24 h. After centrifugation, cells were resuspended in PBS containing propidium iodide (PI, 50 µg/mL) and RNase A (100 µg/mL). After incubation for 30 min at RT in the dark, PI stained cells were analyzed for DNA content in a Gallios Flow Cytometry (Beckman Coulter). The red fluorescence emitted by PI was collected by 620 nm longer pass filter, as a measure of the amount of DNA-bound PI and displayed on a linear scale. Cell cycle distribution was determined on a linear scale. The percentage of cells in cycle phases was determined using the Kaluza Analysis Software (Beckman Coulter).

Cell homogenates preparation. After the incubation with the complexes, the cells were resuspended and homogenized with a cold Tris-mannitol buffer (Tris 2 mM, mannitol 50 mM, pH 7.1, protease inhibitors, and 0.02% sodium azide). Then, the homogenate was disrupted by sonication (15 1-s bursts, 60 W). For lipid peroxidation and protein carbonyl analysis, the homogenate was centrifuged for 10 min at 3,000 g at 4°C and for thioredoxin reductase activity determination, the homogenate was centrifuged for 10 min at 10,000 g at 4°C. The supernatant was taken for the study. Protein content was measured by following the Bradford method (Bio-Rad, Hercules, CA, USA).

Measurement of lipid and protein oxidation. The level of lipid peroxidation was determined by measuring the concentration of malondialdehyde (MDA) and 4- hydroxyalkenals (4-HDA), as described previously.[69] Briefly, MDA+4-HDA reacted with N-methyl-2-phenylindole and yielded a stable chromophore that was measured in a spectrophotometer at 586 nm, using 1,1,3,3-tetramethoxypropane as standard. The results were calculated in nmol MDA+4-HDA mg^{-1} protein. Protein oxidation was analyzed by carbonyl level measurement as previously described.[70] Cell homogenates were incubated with the classical carbonyl reagent 2,4-dinitrophenylhydrazine (DNPH), and protein carbonylation was measured spectrophotometrically at 375 nm. The results were calculated in nmol carbonyl groups mg^{-1} protein.

Thioredoxin reductase activity. Thioredoxin reductase (TrxR) activity was determined by the Thioredoxin Reductase Assay Kit (Sigma-Aldrich, Madrid, Spain) according to the manufacturer's instructions. It is based on the reduction of 5,5´-dithiobis(2-nitrobenzoic) acid (DTNB) with NADPH to 5-thio-2-nitrobenzoic acid (TNB), which produces a strong yellow colour that is measured at 412 nm. The reaction mixture contained 50 µl of the sample, 100 mM potassium phosphate buffer at pH 7.0 with 10 mM EDTA and 0.24 mM NADPH, with and without a TrxR inhibitor, to complete a final volume of 970 µl. The reaction was started by adding 30 µl DTNB (39.6 mg mL^{-1}) and the absorbance change at 412 nm was monitored for 5 min with the spectrophotometer Hitachi U-2800A Spectrophotometer UV-vis Reader. The number of units was calculated by using Beer's Law and an extinction coefficient of 14.150 $M^{-1}cm^{-1}$ for the TNB anion. One unit of TrxR activity is the amount of enzyme catalyzing the reduction of 1 equivalent of DTNB per min at 25 ºC, pH 7 (formation of 2 equivalents of TNB anion). The specific activity of TrxR was calculated as units per mg of total protein.

Mouse model of colitis-associated cancer. All procedures were carried out under Project License PI43/17, approved by the in-house Ethics Committee for Animal Experiments from the University of Zaragoza. The care and use of animals were performed accordingly with the Spanish Policy for Animal Protection RD53/2013, which meets the European Union Directive 2010/63 on the protection of animals used for experimental and other scientific purposes. Female Hsd:ICR (CD-1) mice (16-week-old) were purchased from Envigo (Barcelona, Spain). All mice were housed in Servicio de Experimentación Animal of the Universidad de Zaragoza, Spain, on a 12-hour light/dark cycle with food and water *ad libitum*. Mice were intraperitoneally injected with a single dose of 12 mg/kg azoxymethane (AOM) (Sigma-Aldrich, Madrid, Spain) on day 1, followed by three cycles of dextran sulfate sodium (DSS) MW 40 kDa (Sigma-Aldrich, Madrid, Spain) administration (Each cycle: 3% DSS during 5 days, followed of drinking water during 16 days), and then drinking water until the end of the experiment on week 10-14.

Primary cultures of mouse colonic tumors. Colonic tumors were isolated from the mice treated with the above AOM/DSS protocol (2-3 tumors/mouse) and collected in DMEM medium supplemented with 10% FBS, 100 U/mL penicillin, 100 µg/mL streptomycin, 25 µL/mL antibiotic/antimycotic (100x) and 50 µg/mL gentamycin. Tumors were cut into pieces and processed for enzymatic digestion in culture medium with 5 % FBS supplemented with 2 mM glutamine, insulin 4 µg/mL, dispase I 0.08 mg/mL, collagenase 0.04 mg/mL and EGF 0.01 µg/mL for 3-4 hours at 37°C in rotation. Tissue masses were washed twice, resuspended in complete medium with 25% FBS supplemented with 2 mM glutamine, insulin 4 µg/mL and EGF 0.01 µg/mL, seeded onto 96-well plates at a density of 10^5 cells per well, and incubated for 72 h at 37°C and in 5% CO_2. The medium was changed 72 h after seeding and every two days thereafter. The experiments of apoptosis (detection of phosphatidylserine with Annexin V-FITC) were carried out in the cells 7 days after seeding, following the above protocol.

Statistical Analyses. All results are expressed as means ± the standard error of the mean (SEM) of at least three independent experiments. Statistical comparisons were performed using Student's t-test or one-way ANOVA followed by the Bonferroni posttest and the differences between P-values<0.05 were considered statistically significant. Statistical analyses were carried out using the Prism GraphPad Program (Prism version 4.0, GraphPad Software, San Diego, CA).

CONCLUSIONS

In this work, we describe the synthesis of seven novel thiolate gold(I) complexes with the water soluble phosphane HMPT. After their structural characterization by the typical techniques including X-ray diffraction for complexes **4**, **5** and **8**, we have evaluated some of their physicochemical properties of the ADME-tox profile such as thermal stability, water solubility, lipophilicity, interaction with BSA, and their antiproliferative activity. All of our complexes showed much more cytotoxic activity than cisplatin in A2780 and A2780R cell lines, and analogous studies with Caco-2/TC7 cells pointed the same tendency. This study with Caco-2 showed that the use of HMPT phosphane instead of PTA derivatives implies more antiproliferative effect up to 10 times in some cases. Besides, two of the gold(I) complexes (complex **7** and **8**) are no toxic drugs for considered normal epithelial cells (differentiated Caco-2/TC7 cells). In addition of these studies, their mechanism of action was carefully investigated. Oxidative stress studies revealed that these two complexes induce a strong inhibition of the antioxidant system TrxR and an oxidative damage in membrane lipids. These complexes do not seem to induce apoptosis in undifferentiated cancer Caco-2/TC7 cells through the phosphatidylserine signaling pathway or by the alteration of cell cycle. However, we do detect a phosphatidylserine externalization in the cells from primary cultures of mouse colon tumors, in contrast to the *in vitro* studies, indicating that complexes **7** and **8** induce apoptosis. All of our studies point that complexes **7** and **8** might be promising candidates to use as treatment in colon cancer chemotherapy.

Conflicts of interest

Authors declare no conflicts of interest.

Acknowledgements

This work was partially founded by Gobierno de Aragón (Grupo Reconocido A02_17R) and associated EU Regional Developments Funds. We are very grateful to Dr. José Emilio Mesonero *(Departamento de Farmacología y Fisiología, Universidad de Zaragoza, Spain)* for providing the Caco-2/TC7 cell line. Authors thank to Centro de Investigación Biomédica de Aragón (CIBA), to *Servicio General de Apoyo a la Investigación-SAI, (Universidad de Zaragoza)* and to *Servicios científico-técnicos del ISQCH* for technical assistance, and Torrecid S.A. for a generous donation of $HAuCl_4$.

REFERENCES

1. *Sleisenger and Fordtran's Gastrointestinal and Liver Disease*, *Vol. 1-2*, Elsevier, Philadelphia (PA), 2010.
2. C. R. Boland and A. Goel, *Gastroenterology*, 2010, **138**, 2073-2087.
3. S. K. H. Li and A. Martin, *Trends Mol Med*, 2016, **22**, 274-289.
4. J. Ferlay, I. Soerjomataram, R. Dikshit, S. Eser, C. Mathers, M. Rebelo, D. M. Parkin, D. Forman and F. Bray, *International Journal of Cancer*, 2015, **136**, E359-E386.
5. W. H. Organization, Global facts and figures on cancer (2015), https://www.who.int/en/news-room/fact-sheets/detail/cancer, 2019).
6. C. S. Potten, C. Booth and D. M. Pritchard, *Int J Exp Pathol*, 1997, **78**, 219-243.
7. B. Gustavsson, G. Carlsson, D. Machover, N. Petrelli, A. Roth, H. J. Schmoll, K. M. Tveit and F. Gibson, *Clin Colorectal Cancer*, 2015, **14**, 1-10.
8. R. Rubbiani, B. Wahrig and I. Ott, *J Biol Inorg Chem*, 2014, **19**, 961-965.
9. B. Bertrand and A. Casini, *Dalton Transactions*, 2014, **43**, 4209-4219.
10. E. E. Langdon-Jones and S. J. A. Pope, *Chemical Communications*, 2014, **50**, 10343-10354.
11. I. Ott, *Coordination Chemistry Reviews*, 2009, **253**, 1670-1681.
12. C. F. Shaw, *Chem Rev*, 1999, **99**, 2589-2600.
13. T. Traut-Johnstone, S. Kanyanda, F. H. Kriel, T. Viljoen, P. D. Kotze, W. E. van Zyl, J. Coates, D. J. Rees, M. Meyer, R. Hewer and D. B. Williams, *J Inorg Biochem*, 2015, **145**, 108-120.
14. E. Atrián-Blasco, S. Gascón, M. J. Rodŕiguez-Yoldi, M. Laguna and E. Cerrada, *Inorganic Chemistry*, 2017, **56**, 8562-8579.
15. E. García-Moreno, S. Gascón, E. Atrián-Blasco, M. J. Rodriguez-Yoldi, E. Cerrada and M. Laguna, *European Journal of Medicinal Chemistry*, 2014, **79**, 164-172.
16. E. Garcia-Moreno, S. Gascon, J. A. Garcia de Jalon, E. Romanos, M. J. Rodriguez-Yoldi, E. Cerrada and M. Laguna, *Anticancer Agents Med Chem*, 2015, **15**, 773-782.
17. E. García-Moreno, A. Tomás, E. Atrián-Blasco, S. Gascón, E. Romanos, M. J. Rodriguez-Yoldi, E. Cerrada and M. Laguna, *Dalton Transactions*, 2016, **45**, 2462-2475.
18. E. Vergara, A. Casini, F. Sorrentino, O. Zava, E. Cerrada, M. P. Rigobello, A. Bindoli, M. Laguna and P. J. Dyson, *ChemMedChem*, 2010, **5**, 96-102.
19. E. Vergara, E. Cerrada, C. Clavel, A. Casini and M. Laguna, *Dalton transactions (Cambridge, England : 2003)*, 2011, **40**, 10927-10935.
20. J. C. Lima and L. Rodriguez, *Anticancer Agents Med Chem*, 2011, **11**, 921-928.
21. I. Ott, X. Qian, Y. Xu, D. H. W. Vlecken, I. J. Marques, D. Kubutat, J. Will, W. S. Sheldrick, P. Jesse, A. Prokop and C. P. Bagowski, *Journal of Medicinal Chemistry*, 2009, **52**, 763-770.
22. T. Zou, C. T. Lum, C.-N. Lok, W.-P. To, K.-H. Low and C.-M. Che, *Angewandte Chemie International Edition*, 2014, **53**, 5810-5814.
23. F. Lombardo, R. S. Obach, M. Y. Shalaeva and F. Gao, *J Med Chem*, 2002, **45**, 2867-2876.
24. V. Gandin, A. P. Fernandes, M. P. Rigobello, B. Dani, F. Sorrentino, F. Tisato, M. Björnstedt, A. Bindoli, A.

Sturaro, R. Rella and C. Marzano, *Biochemical Pharmacology*, 2010, **79**, 90-101.
25. S. Gromer, L. D. Arscott, C. H. Williams, Jr., R. H. Schirmer and K. Becker, *J Biol Chem*, 1998, **273**, 20096-20101.
26. F. Saccoccia, F. Angelucci, G. Boumis, M. Brunori, A. E. Miele, D. L. Williams and A. Bellelli, *Journal of inorganic biochemistry*, 2012, **108**, 105-111.
27. A. Bindoli, M. P. Rigobello, G. Scutari, C. Gabbiani, A. Casini and L. Messori, *Coordination Chemistry Reviews*, 2009, **253**, 1692-1707.
28. A. Baker, C. M. Payne, M. M. Briehl and G. Powis, *Cancer Res*, 1997, **57**, 5162-5167.
29. T. C. Karlenius and K. F. Tonissen, *Cancers (Basel)*, 2010, **2**, 209-232.
30. S. Miranda, E. Vergara, F. Mohr, D. de Vos, E. Cerrada, A. Mendía and M. Laguna, *Inorganic Chemistry*, 2008, **47**, 5641-5648.
31. A. Bauer, N. W. Mitzel, A. Schier, H. Schmidbaur and D. W. H. Rankin, *Chemische Berichte*, 1997, **30**, 5.
32. E. H. Kerns and L. Di, in *Lipophilicity Methods*, Elsevier, San Diego, 2008, ch. 23, p. 10.
33. S. J. Berners-Price and A. Filipovska, *Australian Journal of Chemistry*, 2008, **61**, 661-668.
34. M. J. McKeage, S. J. Berners-Price, P. Galettis, R. J. Bowen, W. Brouwer, L. Ding, L. Zhuang and B. C. Baguley, *Cancer Chemotherapy and Pharmacology*, 2000, **46**, 343-350.
35. B. Palazzo, M. Iafisco, M. Laforgia, N. Margiotta, G. Natile, C. L. Bianchi, D. Walsh, S. Mann and N. Roveri, *Advanced Functional Materials*, 2007, **17**, 2180-2188.
36. G. Boscutti, C. Nardon, L. Marchio, M. Crisma, B. Biondi, D. Dalzoppo, L. Dalla Via, F. Formaggio, A. Casini and D. Fregona, *ChemMedChem*, 2018, **13**, 1131-1145.
37. P. L. T, M. Mondal, K. Ramadas and S. Natarajan, *Spectrochim Acta A Mol Biomol Spectrosc*, 2017, **183**, 90-102.
38. V. Anbazhagan and R. Renganathan, *J Lumin*, 2008, **128**, 1454-1458.
39. Y. Moriyama, D. Ohta, K. Hachiya, Y. Mitsui and K. Takeda, *J Protein Chem*, 1996, **15**, 265-272.
40. C. K. Mirabelli, R. K. Johnson, C. M. Sung, L. Faucette, K. Muirhead and S. T. Crooke, *Cancer Res*, 1985, **45**, 32-39.
41. J. R. Lakowicz, in Principles of Fluorescence Spectroscopy, ed. Springer, New York, 3rd ed., 2006, vol. 1, ch. 8, pp. 277-310.
42. J. F. Neault and H. A. Tajmir-Riahi, *Bba-Protein Struct M*, 1998, **1384**, 153-159.
43. T. Mosmann, *J Immunol Methods*, 1983, **65**, 55-63.
44. J. Mesonero, L. Mahraoui, M. Matosin, A. Rodolosse, M. Rousset and E. Brot-Laroche, *Expression or the hexose transporters GLUT1–GLUT5 and SGLT1 in clones of Caco–2 cells*, 1994.
45. V. Meunier, M. Bourrié, Y. Berger and G. Fabre, *Cell Biology and Toxicology*, 1995, **11**, 187-194.
46. M. Rousset, *Biochimie*, 1986, **68**, 1035-1040.
47. E. Guerrero, S. Miranda, S. Lüttenberg, N. Fröhlich, J.-M. Koenen, F. Mohr, E. Cerrada, M. Laguna and A. Mendía, *Inorganic Chemistry*, 2013, **52**, 6635-6647.
48. M. Schieber and Navdeep S. Chandel, *Current Biology*, 2014, **24**, R453-R462.
49. V. Sosa, T. Moliné, R. Somoza, R. Paciucci, H. Kondoh and M. E. Lleonart, *Ageing Research Reviews*, 2013, **12**, 376-390.
50. B. Bertrand, A. Citta, I. L. Franken, M. Picquet, A. Folda, V. Scalcon, M. P. Rigobello, P. Le Gendre, A. Casini and E. Bodio, *J Biol Inorg Chem*, 2015, **20**, 1005-1020.
51. M. Luthman and A. Holmgren, *Biochemistry*, 1982, **21**, 6628-6633.
52. R. Rubbiani, I. Kitanovic, H. Alborzinia, S. Can, A. Kitanovic, L. A. Onambele, M. Stefanopoulou, Y. Geldmacher, W. S. Sheldrick, G. Wolber, A. Prokop, S. Wölfl and I. Ott, *Journal of Medicinal Chemistry*, 2010, **53**, 8608-8618.
53. E. Shacter, Protein oxidative damage in Methods in Enzymology, Academic Press, Elsevier: La Jolla, CA, USA, 2000, Vol. 319,pp. 428-436.
54. D. Gérard-Monnier, I. Erdelmeier, K. Régnard, N. Moze-Henry, J.-C. Yadan and J. Chaudière, *Chemical Research in Toxicology*, 1998, **11**, 1176-1183.
55. M. P. Rigobello, A. Folda, B. Dani, R. Menabò, G. Scutari and A. Bindoli, *European Journal of Pharmacology*, 2008, **582**, 26-34.
56. D. L. Vaux and S. J. Korsmeyer, *Cell*, 1999, **96**, 245-254.
57. V. A. Fadok, D. L. Bratton, S. C. Frasch, M. L. Warner and P. M. Henson, *Cell Death Differ*, 1998, **5**, 551-562.
58. V. A. Fadok, A. de Cathelineau, D. L. Daleke, P. M. Henson and D. L. Bratton, *J Biol Chem*, 2001, **276**, 1071-1077.
59. M. R. Bennett, D. F. Gibson, S. M. Schwartz and J. F. Tait, *Circ Res*, 1995, **77**, 1136-1142.
60. G. M. Cooper, in The cell: a molecular approach, ASM Press, Sunderland (MA), 2nd edn., 2000, ch. 14.
61. I. U. Rehman, Z. Movasaghi and S. Rehman, Vibrational Spectroscopy for Tissue Analysis, CRC Press, CRC Press, Boca Raton (FA), 1st edn., 2012.
62. I. Mármol, M. Virumbrales-Muñoz, J. Quero, C. Sánchez-de-Diego, L. Fernández, I. Ochoa, E. Cerrada and M. J. R. Yoldi, *Journal of inorganic biochemistry*, 2017, **176**, 123-133.
63. M. De Robertis, E. Massi, M. L. Poeta, S. Carotti, S. Morini, L. Cecchetelli, E. Signori and V. M. Fazio, *Journal of carcinogenesis*, 2011, **10**, 9-9.
64. B. Parang, C. W. Barrett and C. S. Williams, in Gastrointestinal Physiology and Diseases: Methods and Protocols, ed. A. I. Ivanov, Springer New York, 2016.
65. R. Uson, A. Laguna, M. Laguna, D. A. Briggs, H. H. Murray and J. P. Fackler, *Inorg. Synth.*, 2007, **26**, 7.
66. L. Farrugia, *Journal of Applied Crystallography*, 1999, **32**, 837-838.
67. J. Mesonero, L. Mahraoui, M. Matosin, A. Rodolosse, M. Rousset and E. Brot-Laroche, *Biochemical Society transactions*, 1994, **22**, 681-684.
68. F. Zucco, A. F. Batto, G. Bises, J. Chambaz, A. Chiusolo, R. Consalvo, H. Cross, G. Dal Negro, I. de Angelis, G. Fabre, F. Guillou, S. Hoffman, L. Laplanche, E. Morel, M. Pincon-Raymond, P. Prieto, L. Turco, G. Ranaldi, M. Rousset, Y. Sambuy, M. L. Scarino, F. Torreilles and A. Stammati, *Altern Lab Anim*, 2005, **33**, 603-618.
69. S. Gonzalo, L. Grasa, M. P. Arruebo, M. A. Plaza and M. D. Murillo, *Neurogastroenterology & Motility*, 2011, **23**, 80-90.
70. E. Latorre, C. Mendoza, E. Layunta, A. I. Alcalde and J. E. Mesonero, *Cell Stress Chaperones*, 2014, **19**, 289-293.

View Article Online
DOI: 10.1039/C9DT04423J